

# ON BLIND EQUALIZATION OF M-ARY BI-ORTHOGONAL SIGNALING

A.G. Klein, C.R. Johnson, Jr.\*

Cornell University  
School of Electrical & Computer Engineering  
Ithaca, NY 14853, USA

P. Duhamel

Supélec/LSS  
3, rue Joliot-Curie  
91192 Gif-sur-Yvette, FRANCE

## ABSTRACT

$M$ -ary bi-orthogonal modulation or  $M$ -ary bi-orthogonal keying (MBOK) is a modulation scheme that has recently been considered for use in several consumer wireless standards, including the IEEE 802.11 WLAN standard and the ultra wideband (UWB) 802.15.3a WPAN standard. In this paper, we propose a novel blind adaptive equalizer for such signals. We then discuss the relation of the algorithm to other blind algorithms and demonstrate its local convergence. Finally, we present some numerical examples that demonstrate its features and performance.

## 1. INTRODUCTION

$M$ -ary bi-orthogonal modulation or  $M$ -ary bi-orthogonal keying (MBOK) is a modulation scheme that has recently been considered for use in several consumer wireless standards, including the IEEE 802.11 WLAN standard [1] and the ultra wideband IEEE 802.15.3a WPAN standard [2]. Though MBOK has been given serious consideration by industry, very little attention has been paid to MBOK by the research community, as evidenced by the dearth of literature on the subject. In the applications where MBOK has been considered, intersymbol interference (ISI) is certainly present, and is viewed to be a serious impairment to acceptable performance. While the optimum detector in ISI is the maximum-likelihood detector, its complexity is usually too high for practical implementation, and thus suboptimal schemes are desirable.

In this paper, we propose a linear blind adaptive equalizer for MBOK. First, we present the equalizer structure and investigate the design equations for the minimum mean-squared error (MMSE) equalizer, as well as the equations for trained and decision-directed (DD) least mean squares (LMS) adaptive algorithms. While the MMSE and LMS equalizers for MBOK follow from straightforward application of Wiener filter theory, our main contribution in this paper is a novel blind algorithm. We will show that the algorithm is locally convergent. After proposing the blind algorithm and discussing its characteristics, we will conclude with several simulations demonstrating its convergence properties and superior performance over DD-LMS. In addition, the simulations show the algorithm can blindly obtain the symbol timing under certain conditions on the underlying bi-orthogonal signal set.

\*Supported in part by Applied Signal Technology, Texas Instruments, and NSF Grants CCF-0310023 and INT-0233127. Correspondence email: agk5@cornell.edu

## 2. SYSTEM MODEL

In MBOK, each symbol consists of  $K \triangleq M/2$  chips and represents  $\log_2 M$  bits. The symbols are drawn from a set of  $K$  orthonormal vectors, and are modulated antipodally to give  $M$  possible symbols. Note that when  $M = 2$ , MBOK reduces to binary phase shift keying (BPSK).

Let  $x[n]$  be a chip-rate sequence of MBOK chips, where the symbols are i.i.d. and a complete symbol is generated at times that are multiples of  $K$ . Thus,  $x[1], x[2], \dots, x[K]$  constitute a complete symbol, for example, drawn from the orthonormal columns of  $\pm \mathbf{S}$  where  $\mathbf{S} \in \mathbb{R}^{K \times K}$  is an orthogonal matrix so that  $\mathbf{S}\mathbf{S}^T = \mathbf{I}$ . By using orthonormal vectors, we are effectively fixing the symbol power to be 1, so the power of the chip-rate process  $x[n]$  becomes a function of  $M$ . Common choices for  $\mathbf{S}$  include the Hadamard matrix [1] and the identity matrix [2]; we will stress the latter.

The process  $x[n]$  has some peculiar properties. The process is not strictly stationary, but it is wide-sense stationary. Furthermore, the chips are uncorrelated, but dependent. Thus,

$$E[x[n]x[n+m]] = \begin{cases} 1/K & m = 0 \\ 0 & m \neq 0 \end{cases} \quad (1)$$

whereas the joint probability

$$P(x[n], x[n+m]) \neq P(x[n])P(x[n+m])$$

unless  $x[n]$  and  $x[n+m]$  are from different symbols, i.e. unless  $\lceil n/K \rceil \neq \lceil (n+m)/K \rceil$ . That (1) is true may come as a surprise at first, but can be proven by using the fact that the symbols are i.i.d., and the fact that the rows of  $\mathbf{S}$  are orthonormal.

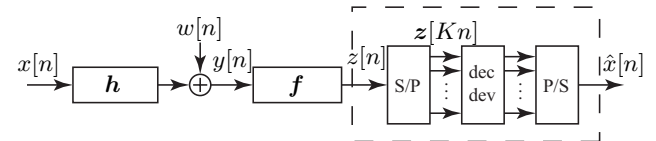


Fig. 1. System Model

The system model is shown in Fig. 1. The MBOK chips are transmitted through a linear time-invariant channel with impulse response  $\mathbf{h} \in \mathbb{R}^{N_h}$  and additive white Gaussian noise  $w[n]$  of variance  $\sigma_w^2$ . The received signal  $y[n]$  is passed through a linear equalizer with impulse response  $\mathbf{f} \in \mathbb{R}^{N_f}$ . Since the decision device must operate in block fashion, we will use a block symbol-rate model to describe the signals. Let  $N_q \triangleq N_f + N_h - 1$  and

let the Hankel matrix  $\mathbf{X}[Kn] \in \mathbb{R}^{N_q \times K}$  contain the transmitted chips as

$$\mathbf{X}[Kn] = \begin{bmatrix} x[Kn] & x[Kn-1] & \dots & x[Kn-K+1] \\ x[Kn-1] & x[Kn-2] & & \ddots \\ \vdots & & & \\ x[Kn-N_q+1] & & & \ddots \end{bmatrix}$$

so the first row of  $\mathbf{X}[Kn]$  contains a complete symbol. Let  $\mathbf{H} \in \mathbb{R}^{N_f \times N_q}$  be the Toeplitz convolution matrix whose rows contain shifted versions of  $\mathbf{h}^\top$ , and let  $\mathbf{W}[Kn] \in \mathbb{R}^{N_f \times K}$  be the Hankel matrix of noise  $w[n]$  defined similarly to the way  $\mathbf{X}[Kn]$  is defined above. Then, the received signal is represented by the Hankel matrix  $\mathbf{Y}[Kn] = \mathbf{H}\mathbf{X}[Kn] + \mathbf{W}[Kn]$  and the output  $\mathbf{z} \in \mathbb{R}^K$  of the equalizer is  $\mathbf{z}[Kn] = \mathbf{Y}^\top[Kn]\mathbf{f}$ . The equalizer output is passed into the decision device. The decision device assumed in this paper is the naïve memoryless Euclidean distance detector, which is essentially a correlation detector [3]. We have chosen this detector for its simplicity and low latency. When the equalizer is operating correctly, the decision device output is

$$\hat{\mathbf{x}}[Kn] \approx [x[Kn - \Delta] \dots x[Kn - \Delta - K + 1]]^\top$$

where  $\Delta$  is the delay through the channel and equalizer, and is a multiple of  $K$ .

### 3. MMSE AND LMS EQUALIZERS

#### 3.1. MMSE Equalizer

Let  $\mathbf{e}_\Delta \in \mathbb{R}^{N_q}$  be the unit vector consisting of a 1 in the  $\Delta$ th location, where  $\Delta$  is a design parameter in this case. The mean-squared error is given by

$$J_m(\mathbf{f}) = E \left[ \|\mathbf{z}[Kn] - \mathbf{X}^\top[Kn]\mathbf{e}_\Delta\|_2^2 \right].$$

Assuming the noise and data are uncorrelated, and using the facts that  $E[\mathbf{X}\mathbf{X}^\top] = \mathbf{I}_{N_q}$  from (1) and for AWGN  $E[\mathbf{W}\mathbf{W}^\top] = K\sigma_w^2\mathbf{I}_{N_f}$ , the orthogonality principle gives the MMSE equalizer

$$\mathbf{f}_m = \left( \mathbf{H}\mathbf{H}^\top + K\sigma_w^2\mathbf{I}_{N_f} \right)^{-1} \mathbf{H}\mathbf{e}_\Delta. \quad (2)$$

It is interesting to note that (2) coincides with the MMSE equalizer for BPSK modulation. Surprisingly, the MMSE equalizer for MBOK is independent of the underlying orthonormal basis vectors  $\mathbf{S}$ . Furthermore,  $K\sigma_w^2$  is exactly the inverse chip SNR since the chip power is  $1/K$  from (1); thus, the MMSE equalizer is also independent of the symbol alphabet size.

#### 3.2. LMS Equalizer

Since the mean-squared error is quadratic, we can use the LMS algorithm to calculate  $\mathbf{f}$  adaptively when training data is available. Taking the instantaneous gradient of the mean-squared error gives the LMS update equation

$$\mathbf{f}_\ell[Kn + K] = \mathbf{f}_\ell[Kn] - \mu\mathbf{Y}[Kn] \left( \mathbf{z}[Kn] - \mathbf{X}^\top[Kn]\mathbf{e}_\Delta \right)$$

where  $\mu$  is a small positive step-size. Note that the presence of  $\mathbf{X}[Kn]$  in the update implies the availability of training data. When training data is unavailable, we can feed back the output of the

decision device  $\hat{\mathbf{x}}[Kn]$  instead, arriving at the DD-LMS update equation

$$\mathbf{f}_d[Kn + K] = \mathbf{f}_d[Kn] - \mu\mathbf{Y}[Kn] (\mathbf{z}[Kn] - \hat{\mathbf{x}}[Kn]).$$

However, DD equalizers are notoriously sensitive to initialization, and generally require an open eye initialization.

#### 3.3. Open Eye Condition

An open eye condition is the situation where the decision device makes no errors in the absence of noise. Unfortunately, the open eye regime for MBOK is in general smaller than the open eye regime for BPSK. The open eye condition for BPSK requires the channel coefficients satisfy  $|h[k]| > \sum_{i \neq k} |h[i]|$  for at least one value of  $k$ . The open eye condition for MBOK will depend on the underlying orthonormal basis vectors  $\mathbf{S}$ , and therefore a simple inequality is not possible. As an example, for an open eye in MBOK with  $M = 4$ ,  $\mathbf{S} = \mathbf{I}_2$ , and  $N_h = 3$ , one of the following 3 conditions must be satisfied

$$\begin{aligned} & \begin{cases} |h[0]| > 2|h[1]| - h[2] \operatorname{sgn}(h[0]) \\ |h[0]| > |h[1]| + |h[2]| \end{cases} \\ \text{or} & \begin{cases} |h[1]| > 2|h[0]| + |h[2]| \\ |h[1]| > |h[0]| + 2|h[2]| \end{cases} \\ \text{or} & \begin{cases} |h[2]| > -h[0] \operatorname{sgn}(h[2]) + 2|h[1]| \\ |h[2]| > |h[0]| + |h[1]| \end{cases} \end{aligned} \quad (3)$$

where  $\operatorname{sgn}$  is the signum function. This is a stricter condition than that for BPSK. Intuition as to why the open eye regime is smaller for MBOK comes about by considering that each symbol consists of  $K$  chips, and thus the allowable channel coefficients for an open eye will have to satisfy a greater number of inequalities to ensure that  $K$  adjacent chips are relatively ISI-free. Decision directed adaptation is generally not a good choice for cold startup of BPSK equalizers, and the situation is only worse for MBOK signals. This motivates a new blind method of equalizer adaptation for MBOK.

### 4. BLIND EQUALIZER

Here, we propose a gradient descent-based blind algorithm. Such algorithms exploit some structure in the transmitted signal, and their cost functions typically depend on higher order statistics; this will be the case for our algorithm. As we pointed out in section 3.1, the second order statistics and hence the MMSE equalizer for an MBOK signal are independent of  $\mathbf{S}$ . However, the fourth-order statistics of  $x[Kn]$  will *not* be independent of  $\mathbf{S}$ , and thus we expect the performance of a candidate algorithm to depend on  $\mathbf{S}$ . It is unreasonable, then, to expect such a blind algorithm to work well for arbitrary choices of  $\mathbf{S}$ . For now, we will consider the case of general  $\mathbf{S}$ , but will later consider the specific choice  $\mathbf{S} = \mathbf{I}$ . This choice of  $\mathbf{S}$  is of interest because it is where our algorithm performs best, and was also the choice considered in the recent UWB proposal [2].

We have defined the MBOK symbols to each have unit norm, so the cost function we choose for the blind algorithm is

$$J_b(\mathbf{f}) = E \left[ (\|\mathbf{z}[Kn]\|_2^2 - 1)^2 \right]. \quad (4)$$

Taking the instantaneous gradient of (4) gives the update equation

$$\mathbf{f}_b[Kn + K] = \mathbf{f}_b[Kn] - \mu\mathbf{Y}[Kn](\mathbf{z}[Kn]^\top \mathbf{z}[Kn] - 1)\mathbf{z}[Kn]$$

While at first glance this simple cost function seems to ignore a lot of structure which is present in the MBOK signal, we show that this is not the case and we draw connections to several other blind algorithms. The form of (4) looks much like the constant modulus algorithm (CMA) [4], and in fact coincides with CMA when  $M = 2$ . The cost function shares even more similarity with Vector CMA [5], though it is distinct in that our algorithm is driven by data that is not i.i.d., and it operates only once every  $K$  chips. Because of these two facts, the cost surface and algorithm performance will be quite different from Vector CMA. Borrowing an idea from [6], and noting that  $\mathbf{z}[Kn] = [z[Kn] \dots z[Kn - K + 1]]^T$ , we see that the cost function can be expanded as

$$J_b(\mathbf{f}) = (1 - K) + \sum_{i=0}^{K-1} E[(z^2[Kn - i] - 1)^2] + \sum_{i=0}^{K-1} \sum_{j=0, j \neq i}^{K-1} E[z^2[Kn - i]z^2[Kn - j]].$$

This gives an interesting interpretation since the second term is exactly the CMA cost when operating chip-by-chip, while the third term represents a penalty of the cross-correlation of the squared equalizer output.

## 5. STABILITY OF ZERO-FORCING SOLUTIONS

To investigate the zero-forcing (ZF) solutions, we first assume that there is no AWGN, so  $\sigma_w^2 = 0$ . We define the combined channel and equalizer response  $\mathbf{q} \triangleq \mathbf{H}^T \mathbf{f} \in \mathbb{R}^{N_q}$ . Recalling that  $E[\mathbf{X}[Kn]\mathbf{X}^T[Kn]] = \mathbf{I}_{N_q}$ , we can expand the cost function (4) as

$$J_b(\mathbf{f}) = E[(\mathbf{q}^T \mathbf{X}[Kn]\mathbf{X}^T[Kn]\mathbf{q})^2] - 2\mathbf{q}^T \mathbf{q} + 1 = \sum_{k, \ell, m, p=0}^{N_q-1} q[k]q[\ell]q[m]q[p]r[k, \ell, m, p] - 2 \left[ \sum_{k=0}^{N_q-1} q^2[k] \right] + 1 \quad (5)$$

where

$$r[k, \ell, m, p] \triangleq \sum_{u, v=0}^{K-1} E \left[ x[Kn - k - u]x[Kn - \ell - u] \cdot x[Kn - m - v]x[Kn - p - v] \right]$$

for  $0 \leq k, \ell, m, p \leq N_q - 1$ . We note that  $r$  has the symmetry properties

$$r[k, \ell, m, p] = r[\ell, k, m, p] = r[k, \ell, p, m] = r[m, p, k, \ell].$$

Another property of  $r$  is that, for any  $\Delta$  that is a multiple of  $K$ ,

$$r[k, \ell, \Delta, \Delta] = \delta[\ell - k]. \quad (6)$$

where  $\delta$  is the Kronecker delta. Due to space limitations, we will not show the proof for (6), but it relies on the facts that  $E[x[n]] = 0$ , the process  $x[n]$  is cyclo-stationary, the symbols are i.i.d., and rows and columns of  $\mathbf{S}$  are orthonormal.

Taking the derivative of (5) gives

$$\frac{1}{4} \frac{\partial J_b(\mathbf{f})}{\partial f[i]} = \sum_{k=i}^{i+N_h-1} h[k-i] \cdot \left[ \underbrace{\left( \sum_{\ell, m, p=0}^{N_q-1} q[\ell]q[m]q[p]r[k, \ell, m, p] \right)}_{\triangleq \Lambda[k]} - q[k] \right] \quad (7)$$

where we have used the symmetry of  $r$  in simplifying the expression. The gradient can be written in matrix form as  $\nabla J_b(\mathbf{f}) = 4\mathbf{H}\mathbf{\Lambda}$  where  $\mathbf{H}$  is the channel matrix and the vector  $\mathbf{\Lambda} \in \mathbb{R}^{N_q}$  is defined in (7). The Hessian is then

$$\frac{1}{4} \frac{\partial^2 J_b(\mathbf{f})}{\partial f[i] \partial f[j]} = \sum_{k=i}^{i+N_h-1} h[k-i] \sum_{\ell=j}^{j+N_h-1} h[\ell-j] \Psi[k, \ell]$$

where

$$\Psi[k, \ell] \triangleq -\delta[\ell - k] + \sum_{m, p=0}^{N_q-1} q[m]q[p] (r[k, \ell, m, p] + 2r[k, p, m, \ell]). \quad (8)$$

The Hessian matrix becomes  $H J_b(\mathbf{f}) = 4\mathbf{H}\mathbf{\Psi}\mathbf{H}^T$  where the non-bold  $H$  denotes the Hessian operator, and the square matrix  $\mathbf{\Psi} \in \mathbb{R}^{N_q \times N_q}$  is defined in (8).

Thus, stationary points come in two varieties: those where  $\mathbf{\Lambda} = \mathbf{0}$  and those where  $\mathbf{\Lambda}$  is in the null space of  $\mathbf{H}$ . We note that there is always a maximum at  $\mathbf{f} = \mathbf{0}$  since for this value of  $\mathbf{f}$  the gradient is zero, and the Hessian is  $-4\mathbf{I}$  which is negative definite.

In BPSK, admissible ZF solutions are those where  $\mathbf{q} \approx e_{\Delta}$  for any  $\Delta$ . In MBOK, however, the chips must be aligned to the symbol boundary before passing through the decision device; thus, we define the ZF solutions as those where  $\Delta$  is a multiple of  $K$ . To analyze the gradient at the ZF solutions, we substitute  $q[n] = \delta[n - \Delta]$  into (7) and use (6) to obtain  $\Lambda[k] = 0$ , and thus  $\nabla J_b(\mathbf{f})|_{\mathbf{q}=e_{\Delta}} = \mathbf{0}$ , so the ZF solutions are stationary points. Now, we need to show that they are minima. Substituting  $q[n] = \delta[n - \Delta]$  into (8) and again using (6) gives

$$\Psi[k, \ell] = 2r[k, \Delta, \Delta, \ell]. \quad (9)$$

Thus far, we have not assumed anything about  $\mathbf{S}$  other than its orthogonality. As mentioned previously, the fourth order terms will depend on the particular choice of  $\mathbf{S}$ , and so the expression  $r[k, \Delta, \Delta, \ell]$  will depend on  $\mathbf{S}$ . We will show the positive definiteness of the Hessian for the particular choice  $\mathbf{S} = \mathbf{I}$ . When  $\mathbf{S} = \mathbf{I}$  and for any  $\Delta$  that is a multiple of  $K$ ,

$$r[k, \Delta, \Delta, \ell] = \begin{cases} 0 & \text{for } k \neq \ell \\ > 0 & \text{for } k = \ell \end{cases}. \quad (10)$$

The proof of this uses the same brute-force machinery as in proving (6). From (9) and (10), we see that  $\mathbf{\Psi}$  reduces to a diagonal matrix of strictly positive values. Since  $\mathbf{H}$  is full row rank and  $\mathbf{\Psi}$  is a diagonal matrix of positive values, the Hessian is positive definite [7]. Thus, we have shown that the algorithm admits the ZF solutions as extrema, and that they are minima in the case when  $\mathbf{S} = \mathbf{I}$ .

## 6. NUMERICAL EXAMPLES

### 6.1. Visualizing the cost surface

For illustration, consider the noiseless case with  $\mathbf{h} = 1$ ,  $N_f = 2$ , and  $\mathbf{S} = \mathbf{I}_2$ , so there are  $K = 2$  chips per symbol. This choice of  $\mathbf{h}$  may seem trivial, but it allows us to focus on the class of minima where  $\mathbf{\Lambda} = \mathbf{0}$  since  $\mathbf{H}$  reduces to the identity matrix. The cost surface is shown in Fig. 2, where we observe the presence of a maximum at the origin and only 2 minima, those at the ZF solution  $\mathbf{q} = \mathbf{f} = \pm[1, 0]^\top$ . It is interesting to note that minima do not also occur at  $\mathbf{q} = \pm[0, 1]^\top$ , as they would for BPSK, but instead there are saddle points in that region. The fact that these are not minima implies that the proposed algorithm can acquire the symbol timing since, as hoped, minima only occur for  $\Delta$  a multiple of  $K$ . If we change the underlying basis vectors so that  $\mathbf{S}$

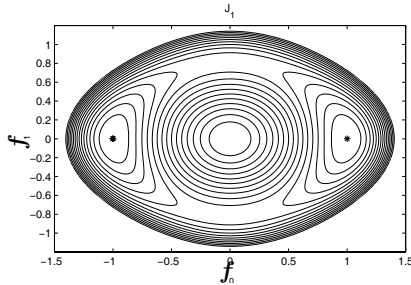


Fig. 2. Cost surface

is the  $2 \times 2$  Hadamard matrix, minima do appear at  $\mathbf{q} = [0, 1]^\top$ . For this choice of  $\mathbf{S}$ , the chip statistics are identical to BPSK since the symbols become  $\pm[1, 1], \pm[1, -1]$ . Thus, when  $\mathbf{S}$  is chosen to be the Hadamard matrix, the algorithm has no hope of recovering the symbol timing since the chips are effectively i.i.d. and so we have the appearance of false minima at undesirable delays.

### 6.2. Approximate Constellation Rotation

We can plot a  $K$ -dimensional symbol constellation by plotting the value of each chip along an axis. The ideal constellation has points at  $(\pm 1, 0)$  and  $(0, \pm 1)$  when  $\mathbf{S} = \mathbf{I}_2$ , for example. The effects of a linear filter on the MBOK symbol constellation conflict with our intuition for more traditional 2-D constellations like quadrature amplitude modulation (QAM). Nevertheless, we know that CMA-like (i.e. dispersion minimization) cost functions are invariant to rotation, and it is interesting to consider what class of impulse responses might cause a constellation rotation in MBOK, and whether our algorithm may exhibit rotational invariance.

It turns out that impulse responses exhibiting perfect arbitrary constellation rotations are not possible, except for the rotation angle  $\theta = \pi$ , which is possible with the one-tap combined response  $\mathbf{q} = -\mathbf{e}_\Delta$ . However, we can find responses that are approximate rotations. The class of impulse responses that best approximate a rotation in the least-squares sense are those of the form  $\mathbf{q} = [\dots, 0, \frac{1}{2} \sin \theta, \cos \theta, -\frac{1}{2} \sin \theta, 0, \dots]^\top$  where there are at most 3 non-zero coefficients. However, as the rotation angle varies, the cluster variance of the rotated constellation oscillates as  $(\sin^2 \theta)/2$ . This implies that rotated constellations with angles near 0 and  $\pi$  are best approximated, and angles near  $\theta = \pm\pi/2$  result in poor approximations to a rotated constellation since the constellation points spread out.

It is interesting to explore whether the algorithm exhibits any false minima, and whether there are any stationary points near  $\mathbf{q} = [\frac{1}{2} \sin \theta, \cos \theta, -\frac{1}{2} \sin \theta]^\top$  for some  $\theta$  that is not a multiple of  $\pi$ . Consider the noiseless case with  $\mathbf{h} = 1$ ,  $N_f = 3$ , and  $\mathbf{S} = \mathbf{I}_2$ . After expanding the cost and analyzing the gradient and Hessian, we find stationary points at the following locations:

$\mathbf{q}^\top$	type
$[0, 0, 0]$	maximum
$[\pm 1, 0, 0], [0, 0, \pm 1]$	minima
$[0, \pm\sqrt{2/3}, 0], [\pm\sqrt{1/3}, 0, \mp\sqrt{1/3}]$	saddle pts
$[\pm\sqrt{1/5}, \pm\sqrt{2/5}, \mp\sqrt{1/5}]$ $[\pm\sqrt{1/5}, \mp\sqrt{2/5}, \mp\sqrt{1/5}]$	degenerate saddle pts

We see again that the minima occur only at the ZF solutions, and that there are not minima at  $\mathbf{q} = \pm[0, 1, 0]^\top$ , as there would be in CMA for BPSK. Furthermore, we see degenerate saddle points that correspond to approximate constellation rotations with  $\theta = \tan^{-1}(\sqrt{2})$ . A degenerate saddle point is one where the Hessian is singular, which implies the cost surface is very flat, and the adaptive algorithm will likely suffer convergence speed problems as it passes through this region. However, for this numerical example we observe no undesirable local minima, and the algorithm will provide convergence to a solution with globally optimally performance.

Simulations confirm that the DD-LMS algorithm is sensitive to initialization, and can fail to equalize the channel. Using the initialization  $\mathbf{f}_{init} = [0.8, -1, -0.1]^\top$ , the blind algorithm converged to the ZF solution  $\mathbf{f}_b = [1, 0, 0]^\top$  while the DD algorithm converged to the closed-eye solution  $\mathbf{f}_d = [0.51, -1.03, -0.07]^\top$ .

## 7. CONCLUSION

We have proposed a novel blind algorithm for the equalization of MBOK signals. We then demonstrated that the algorithm has local convergence to the ZF solutions when  $\mathbf{S} = \mathbf{I}$ , and several examples suggest that the algorithm can obtain the symbol timing blindly as well. Future work could attempt to prove convergence to solutions with globally optimally performance, and could investigate modifications to the algorithm so that it performs well with arbitrary bi-orthogonal signal sets.

## 8. REFERENCES

- [1] M. Webster et al., "Proposal for a high speed PHY for the 2.4 GHz band," IEEE P802.11-98/47, Jan. 1998.
- [2] R. Fisher et al., "DS-UWB physical layer submission to 802.15 task group 3a," IEEE P802.15-04/01373r3, July 2004.
- [3] J.G. Proakis, *Digital Communications*, 4th ed., McGraw-Hill, 2001.
- [4] C.R. Johnson, Jr. et al., "Blind equalization using the constant modulus criterion: A review," *Proc. IEEE*, vol. 86, pp. 1927-1950, Oct. 1998.
- [5] V.Y. Yang and D.L. Jones, "A vector constant modulus algorithm for shaped constellation equalization," *IEEE Signal Processing Lett.*, vol. 5, pp. 89-91, Apr. 1998.
- [6] A. Touzni, et al., "Vector-CM stable equilibrium analysis," *IEEE Signal Processing Lett.*, vol. 7, pp. 31-33, Feb. 2000.
- [7] G. Strang, *Linear Algebra and Its Applications*, 3rd ed., Harcourt Brace Jovanovich, pp. 333, 1988.